Supplemental Material for

CYP26C1 is a hydroxylase of multiple active retinoids and interacts with cellular retinoic acid binding proteins

Guo Zhong, David Ortiz, Alex Zelter, Abhinav Nath, Nina Isoherranen

Departments of Pharmaceutics (GZ, NI) and Medicinal Chemistry (DJO, AN), School of Pharmacy, University of Washington, Seattle, WA, USA and Department of Biochemistry, School of Medicine, University of Washington, Seattle, WA, USA

Supplemental Table 1. Mass spectrometry parameters of MRM scans set for metabolite identification experiments.

	DP (V)	CE (V)
4-OH-, 18-OH- and 16-OH-RA isomers	-80	-28
4-oxo-RA isomers	-95	-22
4-oxo-16-OH- and 4-oxo-18-OH-*at*RA	-90	-25

Note: 70 psi for GS1 and GS2, -2 psi for collision gas (CAD), 35 psi for curtain gas, -10 V for entrance potential (EP) and collision exit potential (CXP), 400°C for temperature (TEM) and -4500 v for ion source.

Supplemental Table 2. Mass spectrometry parameters of MRM scan used in enzyme kinetic experiments.

	MRM transitions	DP (V)	CE (V)	CXP (V)
4-OH-RA isomers	m/z 315 > 253 Da	-80	-28	-7
16-OH-RA isomers	m/z 315 > 241 Da	-80	-28	-7
4-oxo-RA isomers	m/z 313 > 269 Da	-95	-22	-5
4-oxo-*at*RA-d_3	m/z 316 > 272 Da	-100	-10	-5
RA isomers	m/z 299 > 255 Da	-140	-22	-7
4-oxo-16-OH-*at*RA	m/z 329 > 255 Da	-90	-25	-10

Note: 50 psi for GS1, 30 psi for GS2, 9 psi for CAD, 10 psi for curtain gas, -10 V for EP, 400°C for TEM and -4500 v for ion source.

Supplemental Table 3. Homology Model Quality Assessment

Simulation time	Ramachandran % favored/allowed (outlier)	Verify 3D-1D % scores ≥ 0.2	RMSD from CYP120A1 (Å)
Before minimization	80.8 / 11.7 (7.5)	89.6	1.08
After minimization, 0ns	81.0 / 15.0 (4.0)	89.2	1.26
10ns	85.4 / 11.7 (2.9)	94.0	1.34
20ns	86.6 / 11.1 (2.3)	95.0	1.33

Supplemental Table 4. Amino acid residues assigned to secondary structure of CYP26C1 homology model

Secondary Structure	Amino acid residues
A'-helix	T62-V67
A-helix	Q68-Y80
β1-1	V83-H87
β1-2	P92-V96
B-helix	A99-L107
B'-helix	Q119-L125
C-helix	E136-V148
D-helix	E155-A174
β3-1	P178-S180
E-helix	V181-L197
E'-helix	G199-Q206
F-helix	T209-F222
G-helix	S231-H256
H-helix	A266-H272
I-helix	M283-Q314
J-helix	A317-A328
J'-helix	L360-R365
K-helix	R367-L379
β1-4	G386-A390
β1-3	S406-Y409
K'-helix	I411-T417
L-helix	P430-A435
L'-helix	Q462-T479
β3-3	A480-E483
β3-2	R505-P510

Supplemental Table 5. Proposed amino acid residues that interact with RA isomers

Substrate	Active-Site Residues		
	β-ionone Ring	Nonatetraene Chain	Carboxylic Acid Tail
*at*RA	Trp-117, Leu-131, Gly-385, Gly-386, Tyr-387, Pro-496	Leu-89, Pro-118, Ser-120, Leu-125, Leu-221, Phe-222, Phe-299, Ile-497	Leu-221 and Phe-222
9-*cis*-RA	Trp-117, Leu-131, Gly-385, Gly-386, Tyr-387, Pro-496	Leu-89, Pro-118, Ser-120, Leu-125, Leu-221, Phe-222, Phe-295, Phe-299, Ile-497	Leu-221 and Phe-222
13-*cis*-RA	Trp-117, Leu-131, Gly-385, Gly-386, Tyr-387, Pro-496	Leu-89, Pro-118, Ser-120, Leu-125, Leu-221, Phe-222, Phe-299, Ile-497	Ser-120
4-oxo-*at*RA	Trp-117, Leu-125, Leu-131, Pro-496	Leu-89, Pro-118, Ser-120, Leu-125, Leu-221, Phe-222, Phe-295, Phe-299, Ile-497	Leu-221 and Phe-222

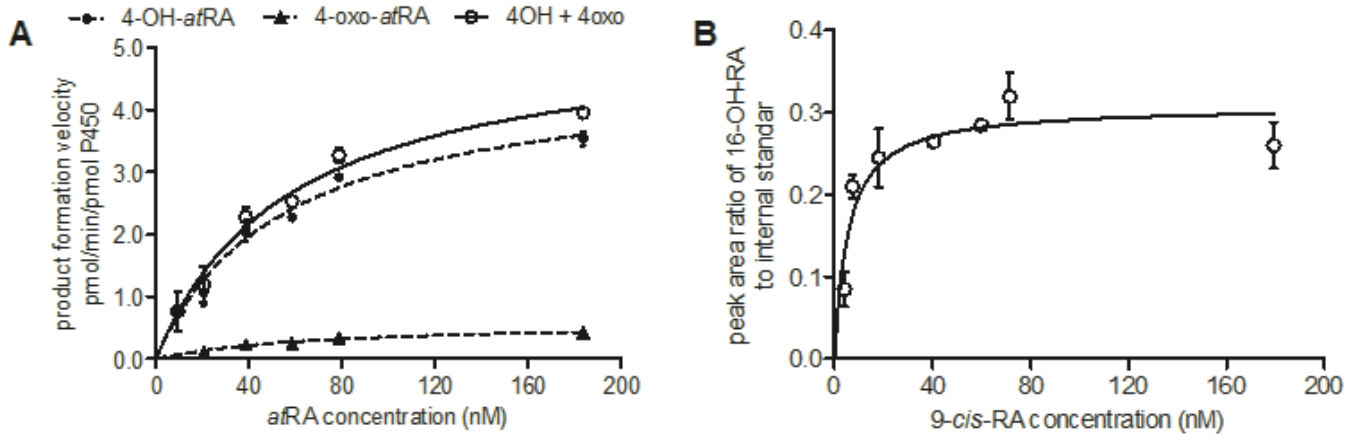

Supplemental Figure 1. Michaelis-Menten plots of metabolite formation. Panel A shows representative metabolite formation of 4-OH-*at*RA (filled circles), 4-oxo-*at*RA (filled triangles) and total 4-OH-*at*RA (open circles). Panel B shows a representative Michaelis-Menten plot of 16-OH-9-cis-RA formation; because of the lack of synthetic 16-OH-9-*cis*-RA, the k_{cat} value was not calculated and the formation of 16-OH-9-*cis*-RA was shown as the peak area ratio of 16-OH-9-*cis*-RA to internal standard.

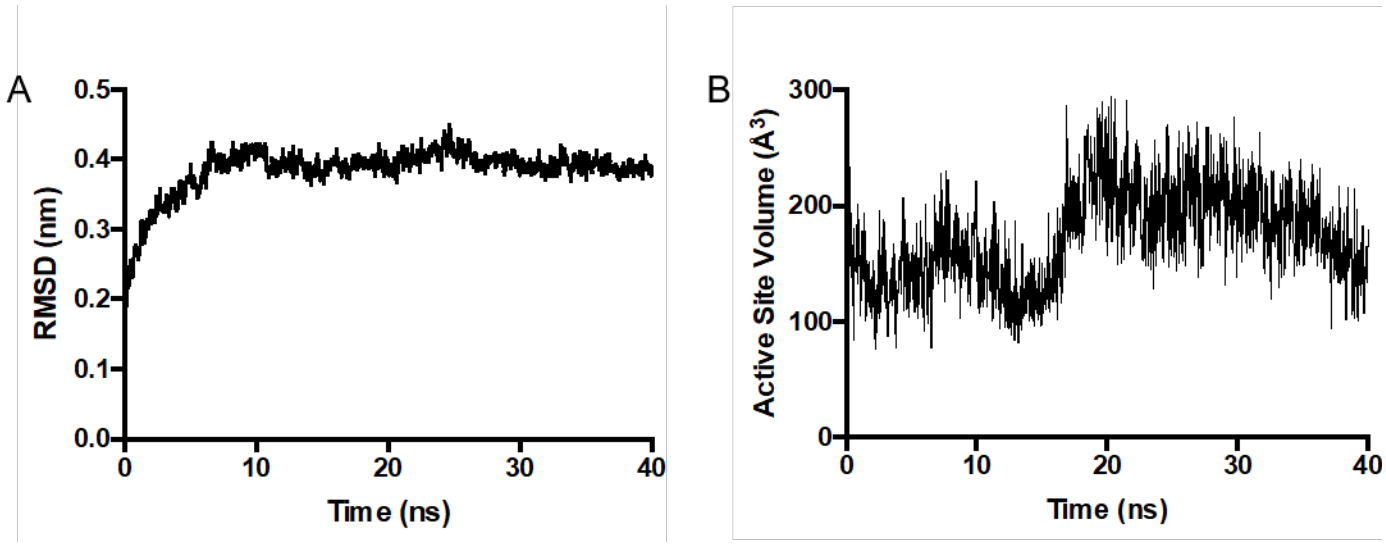

Supplemental Figure 2. RMSD (*Panel A*) and active site volume (*Panel B*) during MD simulations.

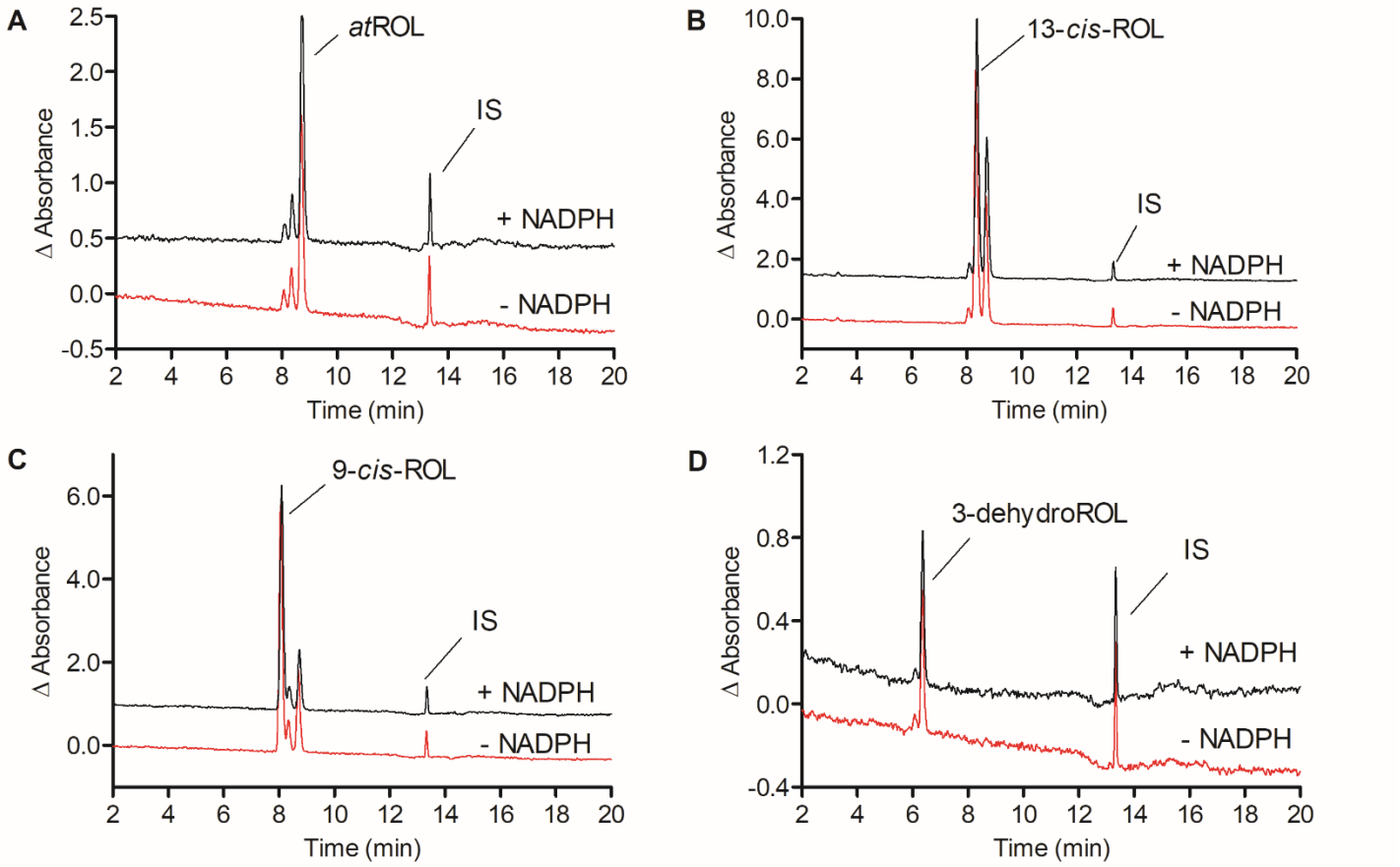

Supplemental Figure 3. LC-UV chromatograms of CYP26C1 incubating with *at*ROL (A), 13-*cis*-ROL (B), 9-*cis*-ROL (C) and 3-dehydroROL (D). Black and red color show the incubation with and without NADPH, respectively. No significant metabolite formation was observed. Based on the ratio of substrate to IS, no significant of substrate depletion was observed.

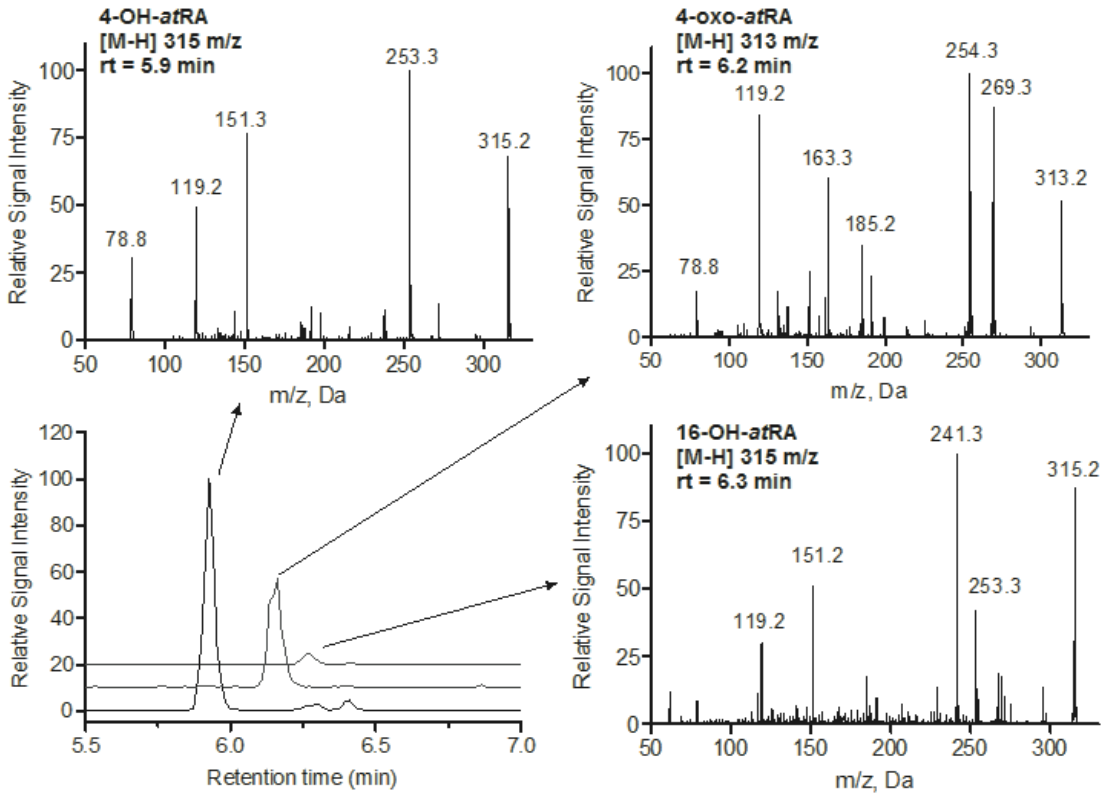

Supplemental Figure 4. MRM chromatogram and MS/MS spectra of *at*RA metabolites formed by CYP26C1. Both the MRM and EPI scan were conducted using a Zorbax C18 column. The corresponding MS/MS spectrum for each peak shown in the MRM chromatogram was indicated by an arrow. The mass values of fragments with the percentage of abundance more than 20% are shown in MS/MS spectra.

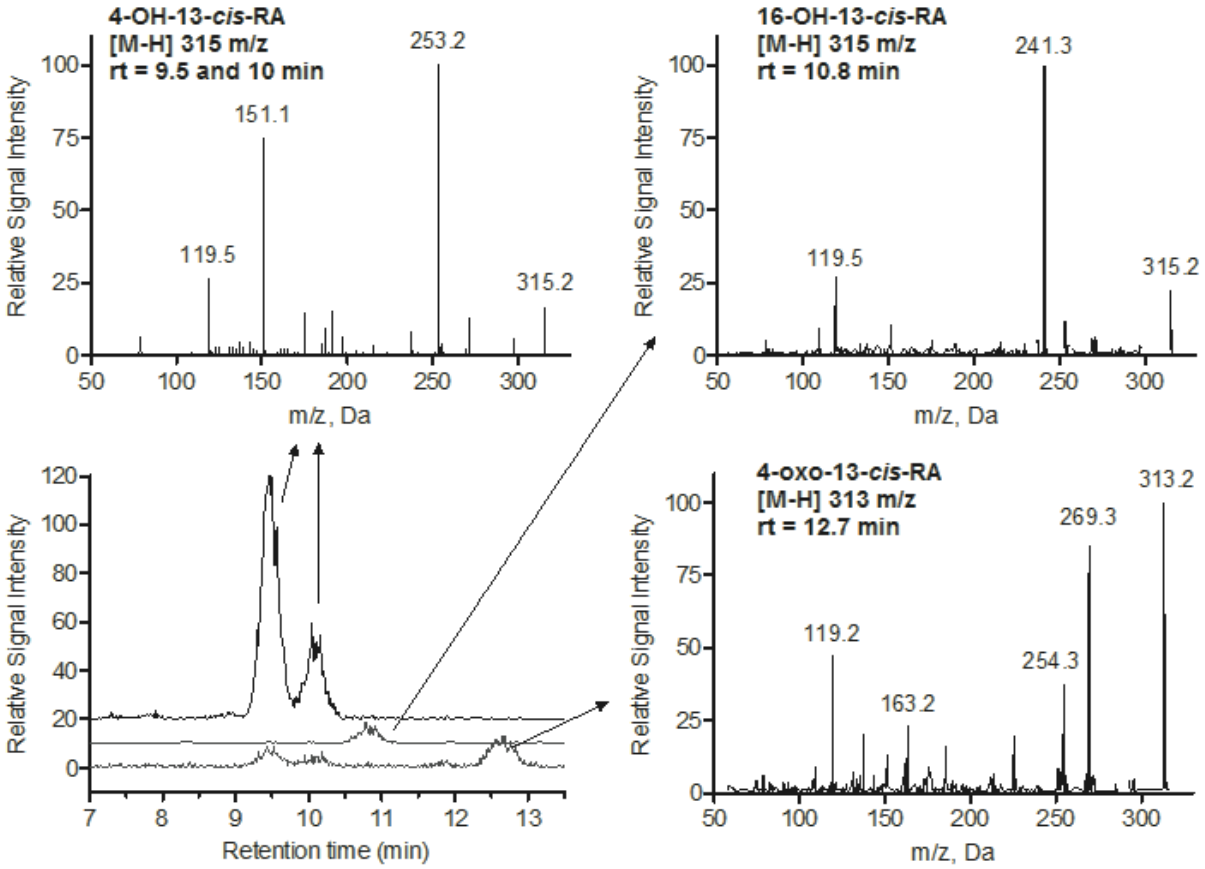

Supplemental Figure 5. MRM chromatogram and MS/MS spectra of 13-*cis*-RA metabolites formed by CYP26C1. Both the MRM and EPI scan were conducted using a Chiracel OD-RH column. The corresponding MS/MS spectrum for each peak shown in the MRM chromatogram was indicated by an arrow. The mass values of fragments with the percentage of abundance more than 20% are shown in MS/MS spectra.

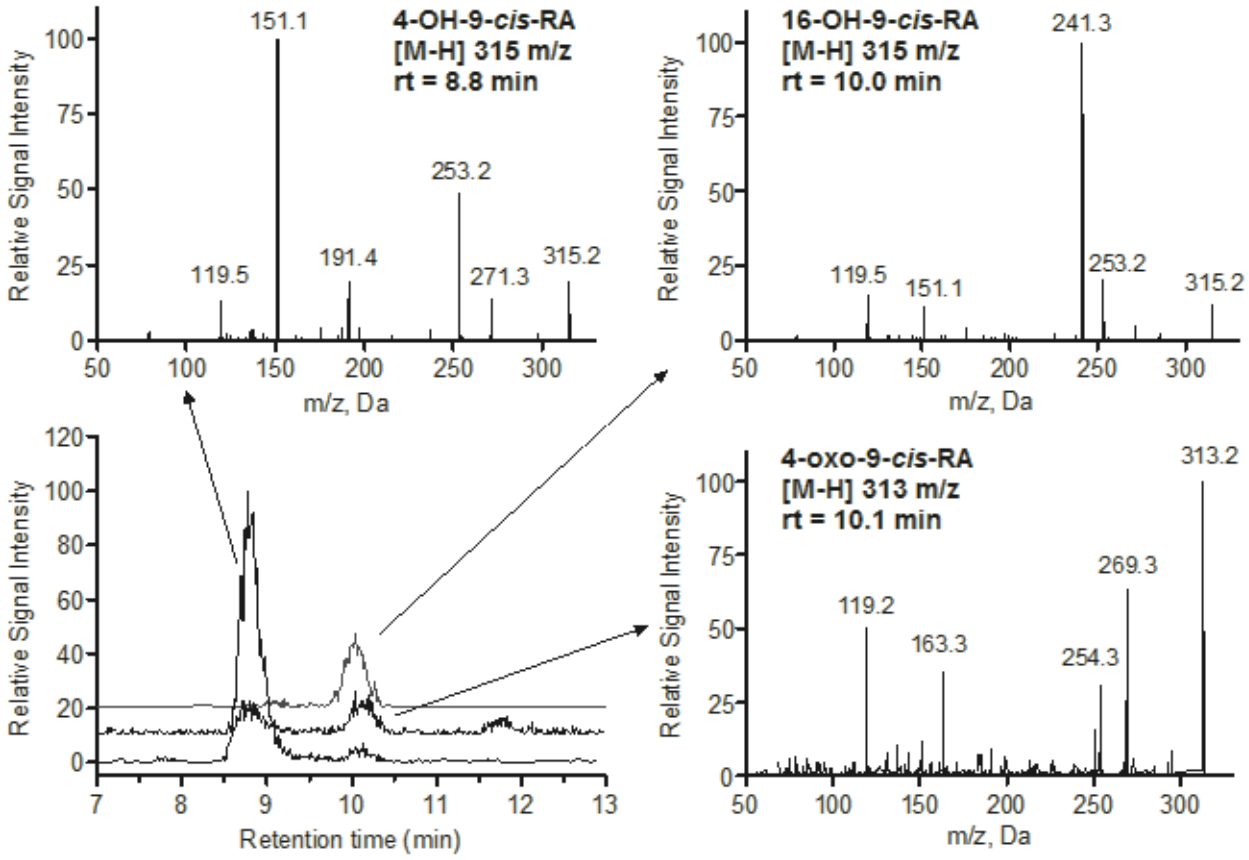

Supplemental Figure 6. MRM chromatogram and MS/MS spectra of 9-*cis*-RA metabolites formed by CYP26C1. Both the MRM and EPI scan were conducted using a Chiracel OD-RH column. The corresponding MS/MS spectrum for each peak shown in the MRM chromatogram was indicated by an arrow. The mass values of fragments with the percentage of abundance more than 20% are shown in MS/MS spectra.